

Nodal Local Cooper Pairs in Multiorbital Systems

Kazumasa Hattori^{1*}, Takuya Nomoto², Takashi Hotta¹, and Hiroaki Ikeda³

¹*Department of Physics, Tokyo Metropolitan University, Minami-osawa, Hachioji, Tokyo 192-0397, Japan*

²*RIKEN Center for Emergent Matter Science (CEMS), Hirosawa, Wako, Saitama 351-0198, Japan*

³*Department of Physics, Ritsumeikan University, Kusatsu, 525-8577, Japan*

We show the emergence of a new class of superconductivity in multiorbital systems, focusing on non-Kramers f^2 states. The Cooper pairs in this class of superconductivity mainly consist of local pairs with the same symmetry as the local f^2 ground states. When the local ground state is an anisotropic representation, the superconducting gap has nodes on the Fermi surface. This nodal superconductivity is mediated by the strong onsite inter-orbital attractions as a consequence of negative- U physics generalized to multiorbital systems. We show that this is indeed realized in a simple two-orbital model with antiferro Hund's coupling and enhanced inter-orbital interaction derived via a systematic local down folding. Finally, we briefly discuss superconductivity in Pr-1-2-20, UBe_{13} , and $PrOs_4Sb_{12}$ in view of the present mechanism.

Unconventional superconductivity (SC) shows various interesting phenomena and has attracted great attention in condensed matter physics. Existence of nodes in their superconducting gap functions is essential for the varieties of phenomena in these unconventional superconductors such as cuprates,¹⁾ ruthenates,²⁾ iron-based pnictides,³⁾ and heavy-fermion superconductors.⁴⁾

Except for the cuprates and some others, the gap functions in many unconventional superconductors have not been fully understood and continued to be under debates, despite intensive experimental and theoretical studies since their discovery. Thus, to unveil their mechanism is a challenging problem in the condensed matter theory.

A promising mechanism for unconventional SC in single band (orbital) systems, fluctuation-mediated SC, has been established by the 80th,⁵⁾ by close analogy with the theory for ³He superfluid.⁶⁾ In particular, intersite fluctuations in the presence of strong local repulsions, typically, such as ferro- or antiferro-magnetic fluctuations, lead to nodal SC. Indeed, many unconventional superconductors have been found in close vicinity of ordered phases.

In recent years, much attention have been paid for multiorbital superconductors, highlighted in iron-based pnictides.³⁾ Some of heavy-fermion superconductors are also attracted renewed interests since after, for example, the discovery of full-gap behavior in the low-temperature specific heat in $CeCu_2Si_2$.⁷⁾ Needless to say, such materials are multiorbital systems. It is now on a stage to clarify the impact of orbital degrees of freedom on SC. Recently, in order to clarify the multiorbital characters in such SC, three of the present authors have classified multipole SC⁸⁾ and discussed that nodal SC can emerge through forming *local* Cooper pairs in multiorbital systems; the pairs are local, but have orbital degrees of free-

dom, which turn into the nodal gap structure.

In this Letter, we show such nodal and local SC can emerge in multiorbital systems and is related to two-electron ground state configurations, when the filling is near two per site. We start first from demonstrating that low-energy effective interactions in such multiorbital models with the spin-orbit interaction (SOI) are completely different from the conventional Hubbard-type parametrization, and include *e.g.*, antiferro Hund's coupling⁹⁾ and enhanced inter-orbital interactions.

Renormalized interactions after integrating out high-energy sectors contain important information for understanding low-energy properties in complex systems. We show a typical example in f -electron (the orbital angular momentum $l = 3$) systems under O_h group, demonstrating the effective local interactions in $j = l - 1/2 = 5/2$

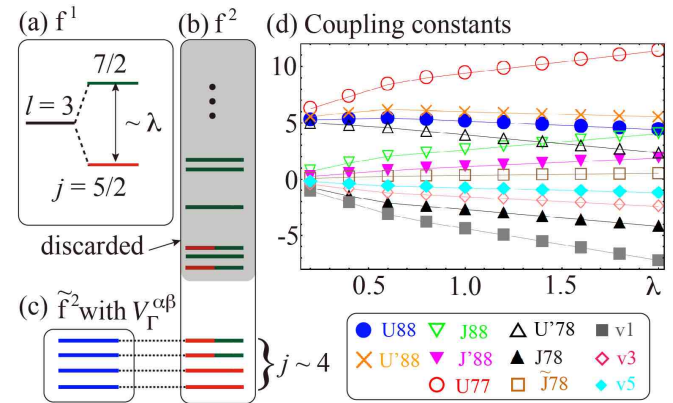


Fig. 1. (Color online) Schematic energy spectra for (a) f^1 , (b) f^2 states. (c) The low-energy effective f^2 states denoted as \tilde{f}^2 . (d) Coupling constants for the effective \tilde{f} system vs λ for $x = 0$, $W = 0.004$, and $(F_0, F_2, F_4, F_6) = (9, 6, 5, 2)$. The unit of energy is eV.

*E-mail: hattori@tmu.ac.jp

multiplets via integrating out $j = l + 1/2 = 7/2$ states that lie in the higher energy of the order of the SOI λ . See Fig. 1(a). This is a kind of down folding,¹⁰⁾ and we call it *local* down folding.

A Hubbard-type model for the $j = 5/2$ orbital has been already analyzed and it turned out impossible to realize Γ_3 nonmagnetic Kramers doublet as ground states for the local two-electron sector (f^2), when considering the conventional Slater integrals $F_{0,2,4,6}$ among the $j = 5/2$ orbitals.¹¹⁾ Thus, when analyzing the Γ_3 as realized in many Pr and U based compounds,¹²⁾ which show quadrupole Kondo effects¹³⁾ and orbital orders,¹²⁾ a simple $j = 5/2$ Hubbard-type model is insufficient. To reconcile the situation, $1/\lambda$ perturbative analysis has been done so far.¹⁴⁾ In this Letter, we show a more rigorous formulation in the realistic parameters (since usually $\lambda \ll$ Hund's coupling), in order to analyze f^2 -based material with the Γ_3 ground states. To this end, we use a method developed in the contractor renormalization group,¹⁵⁾ and obtain the local effective interactions among the low-energy fermions, which are, roughly speaking, $j = 5/2$ states in the case of the filling being nearly two per site. See Figs. 1(a)-(c).

The procedure for calculating the renormalized interactions is as follows. (i) Carry out exact diagonalizations for local Hamiltonian including both $j = 5/2$ and $7/2$ with the Coulomb interactions $F_{0,2,4,6}$ and the SOI under the crystalline-electric-field (CEF) potential expressed by the parameters x and W .¹⁶⁾ Then, one obtains the eigen energy $E_{\Gamma,\alpha}^{(n)}$ for f^n configurations and the corresponding wavefunctions $|f^n \Gamma, \alpha\rangle$, where Γ represents the irreducible representation (irrep) for the O_h group and α runs $1, 2, \dots$ with increasing the energy. For our purpose, only $n \leq 2$ information is needed. Note that the low-energy f^2 states are $j \sim 4$ as predicted by the Hund's rule. (ii) Set target low-energy f^1 states, which belong to Γ_7 or Γ_8 . For realistic parameters, they are almost the $j = 5/2$ states and we denote their creation operators as $\tilde{f}_{\Gamma,7,8}^\dagger$ and ignore the high-energy f^1 states. (iii) Construct f^2 states: $|\tilde{f}^2 \Gamma^{(\alpha)}\rangle = (\tilde{f}^\dagger \tilde{f}^\dagger)_{\Gamma^{(\alpha)}} |0\rangle$, where the states for $\alpha = 1$ consist of two Γ_8 orbitals, while that for $\alpha = 2$ includes at least one Γ_7 orbital:¹⁷⁾ $\Gamma^{(\alpha)} = \Gamma_1^{(1,2)}, \Gamma_3^{(1,2)}, \Gamma_4^{(1)}$, or $\Gamma_5^{(1,2)}$. (iv) Calculate the overlap $r_{\Gamma}^{\alpha\beta} = \langle \tilde{f}^2 \Gamma, \alpha | \tilde{f}^2 \Gamma^{(\beta)} \rangle$. (v) Set the effective Hamiltonian for \tilde{f} 's as

$$H_{\text{eff}} = \sum_{m=7}^8 E_{\Gamma_m,1}^{(1)} \tilde{f}_{\Gamma_m}^\dagger \tilde{f}_{\Gamma_m} + \sum_{\Gamma,\alpha\beta} V_{\Gamma}^{\alpha\beta} |\tilde{f}^2 \Gamma^{(\alpha)}\rangle \langle \tilde{f}^2 \Gamma^{(\beta)}|. \quad (1)$$

Here, $V_{\Gamma}^{\alpha\beta}$ are determined as to (a) maximize the overlap between $|\tilde{f}^2 \Gamma, 1\rangle$ and the ground state of H_{eff} for each Γ : $|\tilde{f}^2 \Gamma\rangle_{gs}$ and (b) reproduce the $E_{\Gamma,\alpha}^{(2)}$ for the first (two) α with nonzero $r_{\Gamma}^{\alpha\beta}$'s for $\Gamma = \Gamma_4(\Gamma_1, \Gamma_3, \Gamma_5)$. To maximize the overlap, one should take $|\tilde{f}^2 \Gamma\rangle_{gs} \propto \sum_{\beta} r_{\Gamma}^{1\beta} |\tilde{f}^2 \Gamma^{(\beta)}\rangle$. H_{eff} thus constructed can reproduce *exactly* the local

spectra up to the two-electron filling. For reproducing f^3, f^4, \dots spectra, one needs three- and four-body interactions and so on. These contributions can be safely ignored, when we are interested in the $f^{0,1,2}$ states.

The symmetry reduces the number of the independent two-body parameters $V_{\Gamma}^{\alpha\beta}$ to ten.¹⁸⁾ The three of them are those in Γ_8 sector: U_{88}, U'_{88}, J_{88} , and J'_{88} with the cubic constraint $U_{88} = U'_{88} - 3J_{88}/4 + J'_{88}$ in V_{88} , where

$$V_{88} = U_{88}(n_{a\uparrow}n_{a\downarrow} + n_{b\uparrow}n_{b\downarrow}) + U'_{88}n_a n_b + J_{88}\mathbf{S}_a \cdot \mathbf{S}_b + J'_{88}(a_{\uparrow}^\dagger a_{\downarrow}^\dagger b_{\downarrow} b_{\uparrow} + \text{H.c.}). \quad (2)$$

Here, we have denoted the annihilation operator for the Γ_8 orbital as $\{a_{\uparrow}, a_{\downarrow}, b_{\uparrow}, b_{\downarrow}\} (\equiv \psi)$, where a and b represents the two kinds of orbital degrees of freedom and $\sigma = \uparrow, \downarrow$ represents the Kramers index. $n_{a\sigma} = a_{\sigma}^\dagger a_{\sigma}$, $n_a = \sum_{\sigma} n_{a\sigma}$, $\mathbf{S}_a = \frac{1}{2} \sum_{\sigma\sigma'} a_{\sigma}^\dagger \vec{\sigma}_{\sigma\sigma'} a_{\sigma'}$ with $\vec{\sigma} = (\sigma^x, \sigma^y, \sigma^z)$ being the Pauli matrices and similar expressions for the b orbital. Denoting the Γ_7 creation operator as c_{σ}^\dagger , $n_7 = \sum_{\sigma} c_{\sigma}^\dagger c_{\sigma}$, and $\mathbf{S}_7 = \frac{1}{2} \sum_{\sigma\sigma'} c_{\sigma}^\dagger \vec{\sigma}_{\sigma\sigma'} c_{\sigma'}$, we obtain the other parts as

$$V_{78} = U_{77}c_{\uparrow}^\dagger c_{\uparrow} c_{\downarrow}^\dagger c_{\downarrow} + U'_{78}n_7 n_8 + J_{78}\mathbf{S}_7 \cdot \mathbf{S}_8 + \tilde{J}_{78}(\tau^z, \tau^x) \cdot \left(\frac{2S_8^z S_7^z - S_8^x S_7^x - S_8^y S_7^y}{\sqrt{3}(S_8^x S_7^x - S_8^y S_7^y)} \right) + [v_1(\psi^\dagger \psi^\dagger)_{\Gamma_1} c_{\uparrow} c_{\downarrow} + \sum_{m=3,5} v_m(\psi^\dagger \psi^\dagger)_{\Gamma_m} (c\psi)_{\Gamma_m} + \text{H.c.}], \quad (3)$$

where $n_8 = n_a + n_b$, $\mathbf{S}_8 = \mathbf{S}_a + \mathbf{S}_b$, and $\vec{\tau} = (\tau^z, \tau^x)$ are the Pauli matrices for the orbital indices $a(b) \rightarrow \uparrow(\downarrow)$.

Figure 1(d) shows various $V_{\Gamma}^{\alpha\beta}$ as a function of λ for the parameters listed in the caption. For real materials, the value of λ is expected to be $\lambda \lesssim 0.5$ eV. The results are summarized as follows.

- $J_{88}, J'_{88} > 0$ and they increase as λ increases.
- $U'_{88} > U_{88}$, i.e., the inter-orbital interaction overwhelms the intra-orbital one for the Γ_8 orbital.
- The complex pair hopping terms (in particular for v_1) are quite large in magnitude.

Note also that the exchange interaction J_{78} between Γ_7 and Γ_8 is ferromagnetic. In addition to the purely electronic origin for such parametrization of the interactions, electron-phonon couplings are known to enhance e.g., antiferro Hund's coupling.^{8,19)}

Now, we discuss that the above results affect the ordering and SC. To capture the essentials, we simplify the full $j = 5/2$ model and introduce an effective model with four-fold degenerate Γ_8 orbital. Although the model is an effective one, and thus, should be regarded as \tilde{f} system in the sense of eq. (1), we will use the notation such as f^n for simplicity. As discussed above, local interactions for the Γ_8 orbital are V_{88} in eq. (2), and then, the f^2 configurations are diagonalized as Γ_1 (1-fold), Γ_3 (2-fold), and Γ_5 (3-fold). Apart from the Γ_8 level, their atomic-limit energy $\epsilon_m^{(2)}$ ($m = 1, 3, 5$) is given as $\epsilon_1^{(2)} = U_{88} + J'_{88}$,

$\epsilon_3^{(2)} = U_{88} - J'_{88}$, and $\epsilon_5^{(2)} = U_{88} + J_{88} - J'_{88}$. Thus, the f^2 ground state is determined by J_{88} and J'_{88} .

We are interested in the situation where the filling $n \equiv \langle n_8 \rangle \sim 2$ per site and the SC emerging there. In a naive mean-field approximation, one decouples the U_{88} term in eq. (2) into a density-density form, while the others into the Cooper channels. The interaction (2) is rewritten as $V_{\text{loc}} = U_{88}n(n-1)/2 + \sum_{m=1,3,5}(\epsilon_m^{(2)} - U_{88})(\psi^\dagger\psi^\dagger)_{\Gamma_m}(\psi\psi)_{\Gamma_m}$, where $(\psi^\dagger\psi^\dagger)_{\Gamma_m}$ indicates the two-electron operator for Γ_m irrep.¹⁷⁾ A mean-field analysis readily leads to SC with local Cooper pairs corresponding to the *atomic CEF ground state* in the f^2 sector $m = m_g$, since the interaction is always attractive $\epsilon_{m_g}^{(2)} - U_{88} < 0$. For this, it is crucial to carry out the decoupling of the U_{88} term not in the Cooper channel but in the density-density one. Physically, if the charge fluctuations are suppressed, the above prescription is expected to be valid and the common energy contribution U_{88} to $\epsilon_m^{(2)}$ is irrelevant. Indeed, in recent dynamical mean-field theory studies on multi-orbital Hubbard models, there appear local *s*-wave SC for $U' > U > 0$,²⁰⁾ and local-triplet SC in a three-orbital model.²¹⁾ These results support the validity of the above prescription. In the following, we will discuss that such SC can be nodal, if realistic hopping parameters reflecting the orbital characters are taken into account.

As an example, let us consider a model on a simple cubic lattice. The non-interacting Hamiltonian is

$$H_0 = \sum_{\mathbf{k}} \psi_{\mathbf{k}\alpha}^\dagger [\epsilon(\mathbf{k}) + \vec{d}(\mathbf{k}) \cdot \vec{\tau} + \vec{\eta}(\mathbf{k}) \cdot \vec{\sigma}\tau^y - \mu]_{\alpha\beta} \psi_{\mathbf{k}\beta}, \quad (4)$$

where μ is the chemical potential, α and β run for the indices $\{1, 2, 3, 4\} \equiv \{a_\uparrow, a_\downarrow, b_\uparrow, b_\downarrow\}$ and \mathbf{k} is the wavenumber and $\vec{\sigma}$ acts on the Kramers indices \uparrow or \downarrow , while τ^y is the y component of the Pauli matrices for the orbital indices. We have used the Einstein contraction for the repeated indices and will use it hereafter. $\epsilon(\mathbf{k})$, $\vec{d}(\mathbf{k})$, and $\vec{\eta}(\mathbf{k})$ are real and they transform as A_{1g} , E_g , and T_{2g} in the O_h group, respectively. The hopping integrals up to the third neighbors are taken into account.²²⁾ In the following analyses, the unit of energy is set to the orbital diagonal nearest-neighbor hopping $t = 1$ and that of length to the lattice constant. The others are set to $(t', t'', d, d', \eta, \eta') = (0.4, 0.1, 0.3, 0.1, 0.1, 0.05)$ as a representative. The one-particle energy $E_{\lambda=1,2}(\mathbf{k})$ is

$$E_\lambda(\mathbf{k}) = \epsilon(\mathbf{k}) + (-1)^\lambda \sqrt{|\vec{d}(\mathbf{k})|^2 + |\vec{\eta}(\mathbf{k})|^2} - \mu, \quad (5)$$

each of which has the Kramers degeneracy. We define the band-based operators as $(\tilde{c}_{\mathbf{k}1\uparrow}, \tilde{c}_{\mathbf{k}1\downarrow}, \tilde{c}_{\mathbf{k}2\uparrow}, \tilde{c}_{\mathbf{k}2\downarrow})^T = [U(\mathbf{k})]^\dagger (a_{\mathbf{k}\uparrow}, a_{\mathbf{k}\downarrow}, b_{\mathbf{k}\uparrow}, b_{\mathbf{k}\downarrow})^T$, where $U(\mathbf{k}) = U(-\mathbf{k})$ is unitary and the superscript T indicates the transpose.

Table I summarizes the band-based (intra band) pair amplitudes $\tilde{\Phi}_{1,2}(\mathbf{k}) = \langle \tilde{c}_{\mathbf{k}1,2\uparrow} \tilde{c}_{-\mathbf{k}1,2\downarrow} \rangle$ induced by a local pair amplitude $\Phi_\Gamma = \langle (\psi_i \psi_i)_\Gamma \rangle$ with \mathbf{i} being the site

Table I. Relation between the local and band-based pair amplitudes. Trivial constant factors are omitted and $\hat{d}_{z,x} = d_{z,x}(\mathbf{k})/D(\mathbf{k})$ and $\hat{\eta}_{x,y,z} = \eta_{x,y,z}(\mathbf{k})/D(\mathbf{k})$, where $D^2(\mathbf{k}) \equiv |\vec{d}(\mathbf{k})|^2 + |\vec{\eta}(\mathbf{k})|^2$ and is invariant under the O_h symmetry. We use the abbreviations $c_{x,y,z} \equiv \cos k_{x,y,z}$ and $s_{x,y,z} \equiv \sin k_{x,y,z}$. In the third column, the functional form for Φ_{Γ_m} is shown (the common factor $1/D(\mathbf{k})$ is omitted for simplicity for $m \geq 3$).

Φ_Γ	$\tilde{\Phi}_\lambda(\mathbf{k})$	functional form
Φ_{Γ_1}	1	1
$\Phi_{\Gamma_{3,u}}$	$\hat{d}_z(\mathbf{k})$	$d(2c_z - c_x - c_y) + d'(2c_x c_y - c_y c_z - c_z c_x)$
$\Phi_{\Gamma_{3,v}}$	$\hat{d}_x(\mathbf{k})$	$\sqrt{3}d(c_x - c_y) + \sqrt{3}d'(c_y c_z - c_z c_x)$
$\Phi_{\Gamma_{5,xy}}$	$\hat{\eta}_z(\mathbf{k})$	$(\eta + \eta' c_z) s_x s_y$
$\Phi_{\Gamma_{5,yz}}$	$\hat{\eta}_x(\mathbf{k})$	$(\eta + \eta' c_x) s_y s_z$
$\Phi_{\Gamma_{5,zx}}$	$\hat{\eta}_y(\mathbf{k})$	$(\eta + \eta' c_y) s_z s_x$

index. For the moment, we do not consider inter-band pairs. Note that due to the local nature of the pair, $\tilde{\Phi}_{1,2}(\mathbf{k}) = \tilde{\Phi}_{1,2}(-\mathbf{k})$ and the symmetry of $\tilde{\Phi}_{1,2}(\mathbf{k})$ is indeed the same as the local order parameter Φ_Γ . Thus, nodal SC is realized when the f^2 ground state is Γ_3 or Γ_5 . The pair is local,²³⁾ and this contrasts with the conventional non-*s*-wave intersite pairs.⁵⁾ The local nature of the SC suggests that it is robust against the detailed changes in the band structure. In a recent paper,²⁴⁾ Bishop et al., also discussed such kinds of SC with nodes, while they introduced attraction in a specific Cooper channel by hands from the beginning.

Now, we examine whether such SC emerges or not. We employ the multiorbital random phase approximation (RPA)^{25,26)} and calculate the transition temperature T_{sc} of SC and T_c for possible multipole orders. Generalized static susceptibilities $\chi_{\gamma\alpha\delta\beta}(\mathbf{q}) \equiv N^{-1} \sum_{\mathbf{k}\mathbf{p}} \int_0^{1/T} d\tau \langle T_\tau \psi_{\mathbf{k}\gamma}^\dagger(\tau) \psi_{\mathbf{k}+\mathbf{q}\delta}(\tau) \psi_{\mathbf{p}\beta}^\dagger(0) \psi_{\mathbf{p}-\mathbf{q}\alpha}(0) \rangle$, where N , T , and T_τ represent the total number of sites, the temperature, and the time-ordered product, respectively, are given in RPA as a recursion equation

$$\chi_{\gamma\alpha\delta\beta}^{\text{RPA}}(\mathbf{q}) = \chi_{\gamma\alpha\delta\beta}^0(\mathbf{q}) - \chi_{\gamma\alpha\alpha'\gamma'}^0(\mathbf{q}) \Gamma_0^{\alpha'\beta'\delta'\gamma'} \chi_{\beta'\delta'\alpha\beta}^{\text{RPA}}(\mathbf{q}). \quad (6)$$

Here, $\chi_{\gamma\alpha\delta\beta}^0(\mathbf{q}) \equiv -TN^{-1} \sum_{\omega\mathbf{k}} G_{\beta\gamma}^0(\omega, \mathbf{k}) G_{\alpha\delta}^0(\omega, \mathbf{k} + \mathbf{q})$ with the Matsubara frequency ω_ℓ and $G_{\alpha\beta}^0(\omega_\ell, \mathbf{k}) = \sum_{\lambda\sigma} U_{\alpha,\lambda\sigma}(\mathbf{k}) U_{\beta,\lambda\sigma}^*(\mathbf{k}) / [i\omega_\ell - E_\lambda(\mathbf{k})]$. For convenience, antisymmetrized interactions $\Gamma_0^{\alpha\beta\delta\gamma}$ have been introduced and eq. (2) is rewritten as $V_{\text{loc}} = \frac{1}{4} \Gamma_0^{\alpha\beta\delta\gamma} \psi_\alpha^\dagger \psi_\beta^\dagger \psi_\delta \psi_\gamma$ with $\Gamma_0^{\alpha\beta\delta\gamma} = V_0^{\alpha\beta\delta\gamma} - V_0^{\alpha\beta\gamma\delta} - V_0^{\alpha\delta\gamma\beta} + V_0^{\beta\alpha\gamma\delta}$, where $V_0^{\alpha\beta\delta\gamma}$ is the interactions (2).²⁷⁾ The effective RPA interactions $V_{\text{eff}}^{\alpha\beta\delta\gamma}$ between Cooper pairs read

$$V_{\text{eff}}^{\alpha\beta\delta\gamma}(\mathbf{q}) = \frac{1}{2} \Gamma_0^{\alpha\beta\delta\gamma} - \Gamma_0^{\alpha'\beta'\delta'\gamma'} \chi_{\beta'\delta'\alpha'\gamma'}^{\text{RPA}} \Gamma_0^{\alpha'\beta\delta\gamma'}, \quad (7)$$

and they are used for calculating T_{sc} in the BCS approximation. All the calculations shown below are done for $N = 64^3$ and 1024 τ bins and $J_{88}, J'_{88} > 0$, which correspond to the Γ_3 ground states in the f^2 sector.

Figure 2(a) shows J_{88} and J'_{88} dependence of T_{sc} and

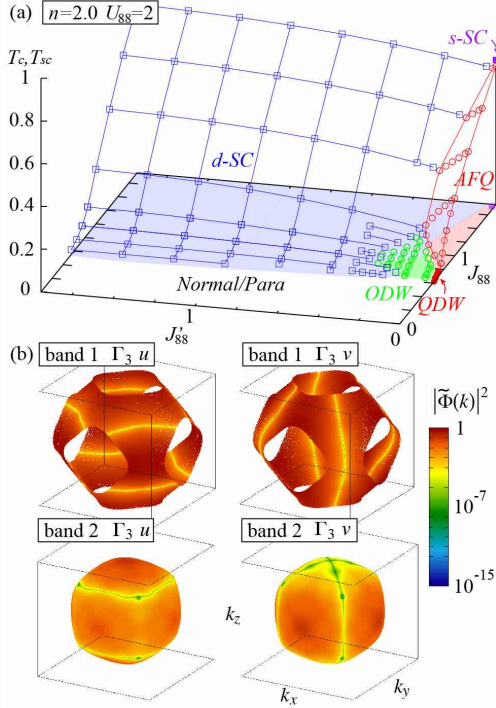


Fig. 2. (Color online) (a) Transition temperatures T_{sc} and T_c in J_{88} - J'_{88} plane. (b) The Fermi surfaces for the band 1 and 2 for $(J_{88}, J'_{88}) = (0.75, 1.0)$ and $T \simeq T_{sc} = 0.06$. The color map represents $|\Phi_{1,2}(\mathbf{k})|^2$ on the FS.

T_c for $U_{88} = 2.0$ and $n = 2.0$. Note that we have not calculated T_{sc} in ordered phases below T_c . For a wide range of parameter space, SC with E_g symmetry (d -SC) appears. This is nearly local SC induced by the renormalized interactions as will be demonstrated below. Thus, our naive analysis is qualitatively valid within the RPA level. The Fermi surfaces (FSs) for $(J_{88}, J'_{88}) = (0.75, 1.0)$ and $T \sim T_{sc}$ are shown in Fig. 2 (b) with the d -wave amplitudes $|\Phi(\mathbf{k})|^2$. Line nodes exist on the both FSs, whose functional forms are qualitatively consistent with the list in Table I. Below T_{sc} , when the chiral combination of the two components are realized in favor of opening the gaps on the FSs, point nodes exist around [111] directions. For larger J_{88} and J'_{88} , the T_{sc} is very high $\sim O(1)$, which means the attraction is too large to be handled in RPA. There, the pairs are extremely local, and thus, the Bose-Einstein condensation of local pairs must occur²⁸⁾ and band off-diagonal pairs exist.

For smaller J'_{88} , three ordered states appear: an antiferro E_g -quadrupole order (AFQ) with the ordered wavenumber $\mathbf{q} = (\pi, \pi, \pi)$, E_g -quadrupole density wave (QDW), and an A_{2u} -octupole density wave (ODW) both with $\mathbf{q} \simeq (\pi, \pi, \pi \pm 0.4\pi)$ and the equivalent directions.

For $J'_{88} \ll J_{88}$ and $J_{88} \simeq U_{88}$, another SC with A_{1g} irrep (s -SC) emerges. This is related to the SC realized for $J'_{88} < 0$, where the ground state for the f^2 sector is Γ_1 . The Γ_1 ground state, according to Table I, leads to A_{1g} Cooper pairs. As for the case of Γ_5 f^2 ground state with $J_{88} < 0$, we expect SC with T_{2g} irrep, while this is not

realized for $U_{88} = 2.0$, since an antiferromagnetic order takes place first. However, for larger $|J_{88}|$, the leading SC instability is the expected T_{2g} type,²¹⁾ and thus, we conclude that our naive argument holds in the RPA results, concerning the dominant superconducting instability.

In order to analyze the d -SC in more details, we show the averaged real-space amplitude

$$\overline{|\Phi(r)|} \equiv \frac{1}{N^3 n_r} \sum_{\mathbf{i}, \mathbf{j}} \sum_{\alpha, \beta} |\langle \psi_{i\alpha} \psi_{j\beta} \rangle| \delta_{|\mathbf{i}-\mathbf{j}|, r}, \quad (8)$$

for two sets of parameters of (J_{88}, J'_{88}) in Fig. 3(a), where n_r is the number of site-pairs with the distance r . Both for $J_{88} = 0.75$ and 1.75 , the order parameter is largest for $r = 0$. For the larger J_{88} , the decay is much steeper. In the inset of Fig. 3(a), the averaged effective interactions

$$\overline{|V_{\text{eff}}(\mathbf{r})|} \equiv \frac{1}{256} \sum_{\alpha\beta\gamma\delta} |V_{\text{eff}}^{\alpha\beta\delta\gamma}(\mathbf{r})|, \quad (9)$$

along the three symmetric directions [001], [110], and [111] are shown. Here, $V_{\text{eff}}(\mathbf{r})$ is the inverse-Fourier transform of eq. (7). As expected from the behavior of $\overline{|\Phi(r)|}$, the effective interactions decay exponentially and the decay rate is faster for the larger J_{88} . The profile of the local part of V_{eff} is a key to gaining the insight into the mechanism for the d -SC. Figure 3(b) demonstrates that $J_{88\text{eff}}$ and $J'_{88\text{eff}}$ [the notation is obvious extension of eq. (2)] grow as increasing J_{88} . This stabilizes the f^2 Γ_3 configuration, leading to the local Cooper pairs with E_g irrep.

Let us provide a few comments on the electron filling n and the band parameter dependence of the phase diagram. As n decreases, all the ordered states including the SC are suppressed due to the decrease in the density of states on the FSs. For $U_{88} = 2.0$ and $n = 1.0$, there are no symmetry broken phases in the present calculations. We have also examined T_{sc} for several sets of the band parameters. The results are qualitatively the same as those shown above and this means that the details of the band parameters and any specific fluctuations play no role for realizing the d -SC discussed in this study.

Finally, we discuss possible application to real materials. Our focus in this Letter is on the Γ_3 ground states in the f^2 configurations under a cubic symmetry, which are realized, *e.g.*, in Pr-based 1-2-20 compounds and SC is found in various systems.¹²⁾ Since the nodal local SC discussed above does not need any specific fluctuation, if SC under high pressure far away from the orbital ordered phase is realized,²⁹⁾ it is a good candidate for it. Another candidate is classical heavy-fermion superconductor UBe_{13} .³⁰⁾ A possible ground state to explain the anomalous normal state is Γ_3 . It is suggested that there are point nodes around [111] directions.³¹⁾ The chiral d -wave state of local pairs suggested above can provide a key clue to understanding the enigmatic superconductivity of UBe_{13} . As for a material with Γ_1 ground states, it is argued that $\text{PrOs}_4\text{Sb}_{12}$ is an s -wave superconductor.³²⁾

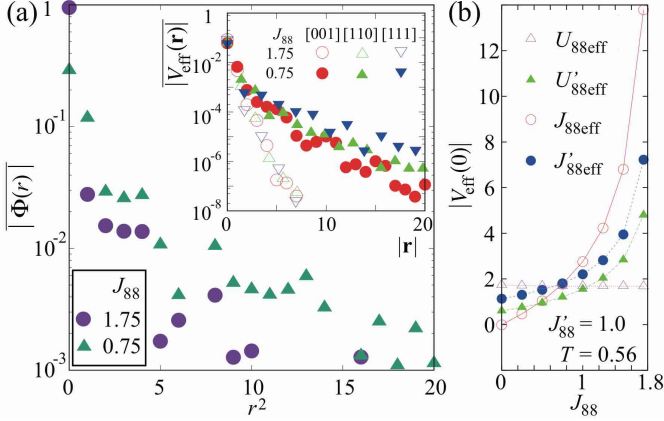


Fig. 3. (Color online) (a) Real space pair amplitude $|\overline{\Phi(r)}|$ as a function of the distance r^2 for $(J_{88}, J'_{88}) = (0.75, 1.0)$ and $(1.75, 1.0)$. Inset: $|V_{\text{eff}}(\mathbf{r})|$ vs $|\mathbf{r}|$ for the direction parallel to [001], [110], and [111]. (b) $V_{\text{eff}}(0)$ for $J'_{88} = 1.0$ and $T = 0.56$ as a function of J_{88} . The effective interactions are evaluated in the normal state, ignoring the presence of T_{sc} (if it exists) for $T > 0.56$.

This is indeed consistent with our theory and it is worth examining the heavy-fermion SC in our future studies.

In summary, we have demonstrated that nodal local superconductivity can appear in multiorbital systems. The nodal structures reflect the local two-electron ground state. We have also derived the effective model by local down folding and found the antiferro Hund's coupling and enhanced inter-orbital interactions, which are the keys to realizing the nodal local superconductivity.

Acknowledgment: This work is supported by a Grant-in-Aid for Scientific Research [Grant No. 16H01079, 16H01081, 16H04017, and 16H04021] from the Japan Society for the Promotion of Science.

- 1) W. E. Pickett, Rev. Mod. Phys. **61**, 433 (1989).
- 2) A. P. Mackenzie and Y. Maeno, Rev. Mod. Phys. **75**, 657 (2003).
- 3) K. Ishida, Y. Nakai, and H. Hosono, J. Phys. Soc. Jpn. **78**, 062001 (2009).
- 4) G. R. Stewart, Rev. Mod. Phys. **73**, 797 (2001).
- 5) K. Miyake, S. Schmidt-Rink, and C. M. Varma, Phys. Rev. B **34**, 6554(R) (1986), D. Scalapino, E. Loh, Jr., and J. E. Hirsch, Phys. Rev. B **34**, 8190(R) (1986).
- 6) A. J. Leggett, Rev. Mod. Phys. **47**, 331 (1975).
- 7) S. Kittaka, et al., Phys. Rev. Lett. **112**, 067002 (2014).
- 8) T. Nomoto, K. Hattori, and H. Ikeda, Phys. Rev. B **94**, 174513 (2016).
- 9) S. Yotsuhashi, H. Kusunose, and K. Miyake, J. Phys. Soc. Jpn. **71**, 389 (2002), K. Hattori, S. Yotsuhashi, and K. Miyake, J. Phys. Soc. Jpn. **74**, 839 (2005),
- 10) F. Aryasetiawan, et al., Phys. Rev. B **70**, 195104 (2004).
- 11) T. Hotta and K. Ueda, Phys. Rev. B **67**, 104518 (2003).
- 12) See a recent review for Pr-based 1-2-20 compounds and ref-

erences therein, T. Onimaru and H. Kusunose, J. Phys. Soc. Jpn. **85**, 082002 (2016).

- 13) D. L. Cox, Phys. Rev. Lett. **59**, 1240 (1987).
- 14) T. Hotta and H. Harima, J. Phys. Soc. Jpn. **75**, 124711 (2006).
- 15) C. J. Morningstar and M. Weinstein, Phys. Rev. D **54**, 4131 (1996).
- 16) $Wx = 15B_4^0$ and $W(1 - |x|) = 180B_6^0$, where $B_{4,6}^0$ are the

CEF parameter for $l = 3$ orbitals. See Ref. 14 and K. R. Lea, M. J. M. Leask, and W. P. Wolf, J. Phys. Chem. Solids **23**, 1381 (1962).

- 17) Definitions of the two-particle products:
 $(\psi^\dagger \psi^\dagger)_{\Gamma_1} = (a_\downarrow^\dagger a_\uparrow^\dagger + b_\downarrow^\dagger b_\uparrow^\dagger)/\sqrt{2}$, $(\psi^\dagger \psi^\dagger)_{\Gamma_{5xy}} = (a_\downarrow^\dagger b_\uparrow^\dagger + a_\uparrow^\dagger b_\downarrow^\dagger)/\sqrt{2}$,
 $(\psi^\dagger \psi^\dagger)_{\Gamma_{5yz}} = (a_\downarrow^\dagger b_\uparrow^\dagger - a_\uparrow^\dagger b_\downarrow^\dagger)/\sqrt{2}$, $(\psi^\dagger \psi^\dagger)_{\Gamma_{5zx}} = i(a_\downarrow^\dagger b_\uparrow^\dagger + a_\uparrow^\dagger b_\downarrow^\dagger)/\sqrt{2}$,
 $(\psi^\dagger \psi^\dagger)_{\Gamma_{3u}} = (a_\downarrow^\dagger a_\uparrow^\dagger - b_\downarrow^\dagger b_\uparrow^\dagger)/\sqrt{2}$, $(\psi^\dagger \psi^\dagger)_{\Gamma_{3v}} = (a_\downarrow^\dagger b_\uparrow^\dagger - a_\uparrow^\dagger b_\downarrow^\dagger)/\sqrt{2}$,
 $(\psi^\dagger c^\dagger)_{\Gamma_{3u}} = (-a_\downarrow^\dagger c_\uparrow^\dagger + a_\uparrow^\dagger c_\downarrow^\dagger)/\sqrt{2}$, $(\psi^\dagger c^\dagger)_{\Gamma_{3v}} = (b_\downarrow^\dagger c_\uparrow^\dagger - b_\uparrow^\dagger c_\downarrow^\dagger)/\sqrt{2}$,
 $(\psi^\dagger c^\dagger)_{\Gamma_{4x}} = [(n_- \psi_\downarrow^\dagger) c_\downarrow^\dagger - (n_- \psi_\uparrow^\dagger) c_\uparrow^\dagger]/\sqrt{2}$,
 $(\psi^\dagger c^\dagger)_{\Gamma_{4y}} = i[(n_+ \psi_\downarrow^\dagger) c_\downarrow^\dagger + (n_+ \psi_\uparrow^\dagger) c_\uparrow^\dagger]/\sqrt{2}$,
 $(\psi^\dagger c^\dagger)_{\Gamma_{4z}} = (a_\downarrow^\dagger c_\uparrow^\dagger + a_\uparrow^\dagger c_\downarrow^\dagger)/\sqrt{2}$, $(\psi^\dagger c^\dagger)_{\Gamma_{5xy}} = (b_\downarrow^\dagger c_\uparrow^\dagger + b_\uparrow^\dagger c_\downarrow^\dagger)/\sqrt{2}$,
 $(\psi^\dagger c^\dagger)_{\Gamma_{5yz}} = [-(m_- \psi_\downarrow^\dagger) c_\downarrow^\dagger + (m_- \psi_\uparrow^\dagger) c_\uparrow^\dagger]/\sqrt{2}$,
 $(\psi^\dagger c^\dagger)_{\Gamma_{5zx}} = i[(m_+ \psi_\downarrow^\dagger) c_\downarrow^\dagger + (m_+ \psi_\uparrow^\dagger) c_\uparrow^\dagger]/\sqrt{2}$,
 where $\mathbf{n}_\pm = (\cos \frac{2\pi}{3}, \pm \sin \frac{2\pi}{3})$, $\mathbf{m}_\pm = (-\sin \frac{2\pi}{3}, \pm \cos \frac{2\pi}{3})$
 and the product means $(\mathbf{n}_\pm \psi_\sigma^\dagger) = \cos \frac{2\pi}{3} a_\sigma^\dagger \pm \sin \frac{2\pi}{3} b_\sigma^\dagger$ and
 similarly $(\mathbf{m}_\pm \psi_\sigma^\dagger) = -\sin \frac{2\pi}{3} a_\sigma^\dagger \pm \cos \frac{2\pi}{3} b_\sigma^\dagger$.

- 18) In addition to the interaction part, one needs to renormalize *e.g.*, hopping terms.¹⁵⁾ However, these depend on the configurations and generate so-called correlated hopping terms. This cannot properly be taken into account in RPA calculations, while it is possible to compile them into *e.g.*, continuous-time quantum Monte Carlo for dynamical-mean-field analysis.
- 19) Y. Nomura, et al., Sci. Adv. **1**, 1500568 (2015), S. Hoshino and P. Werner, Phys. Rev. Lett. **118**, 177002 (2017).
- 20) A. Koga and P. Werner, Phys. Rev. B **91**, 085108 (2015).
- 21) S. Hoshino and P. Werner, Phys. Rev. Lett. **115**, 247001 (2015).
- 22) $\epsilon(\mathbf{k}) = -2t \sum_l c_l - 4t' \sum_l c_m c_n - 8t'' c_x c_y c_z$, ($l, m, n = \text{cyclic}$),
 $\vec{d}(\mathbf{k}) = [d_z(\mathbf{k}), d_x(\mathbf{k})] = [d(2c_z - c_x - c_y) + d'(2c_x c_y - c_y c_z - c_z c_x), \sqrt{3}d(c_x - c_y) + \sqrt{3}d'(c_y c_z - c_z c_x)]$, $\eta(\mathbf{k}) = (\eta + \eta' c_l) s_m s_n$, ($l, m, n = \text{cyclic}$), where $t, t', t'', d, d', \eta, \eta'$ are parameters and $c_l = \cos k_l$ and $s_l = \sin k_l$ ($l = x, y, z$).
- 23) Note that the pair is local in terms of the local bases a and b , while spreads in terms of the band bases.
- 24) C. B. Bishop, et al., Phys. Rev. B **93**, 224519 (2016).
- 25) T. Takimoto, Phys. Rev. B **62**, R14641 (2000).
- 26) T. Takimoto, et al., J. Phys.: Condens. Matter **14**, L369-L375 (2002).
- 27) $V^{\alpha\beta\delta\gamma}$ have nonvanishing elements only in $V_0^{1221} = V_0^{3443} = U_{88}$, $V_0^{1331} = V_0^{2442} = U'_{88} + J_{88}/4$, $V_0^{1441} = V_0^{2332} = U'_{88} - J_{88}/4$, $V_0^{1432} = V_0^{2341} = J_{88}/2$, and $V_0^{1243} = V_0^{3421} = J'_{88}$. Note that $\Gamma_0^{\alpha\beta\gamma\delta} = -\Gamma_0^{\alpha\beta\delta\gamma} = -\Gamma_0^{\beta\alpha\gamma\delta} = \Gamma_0^{\beta\alpha\delta\gamma}$.
- 28) P. Nozières and S. Schmitt-Rink, J. Low Temp. Phys. **59**, 195 (1985).
- 29) K. Matsubayashi, et al., Phys. Rev. Lett. **109**, 187004 (2012).
- 30) H. R. Ott, et al., Phys. Rev. Lett. **50**, 1595 (1983).
- 31) Y. Shimizu, et al., Phys. Rev. Lett. **114**, 147002 (2015).
- 32) N. A. Frederick, et al., Phys. Rev. B **69**, 024523 (2004).